Enhanced fire behavior of Casico - based foams

Vera Realinho, Marcelo Antunes, José Ignacio Velasco*

Centre Català del Plàstic, Departament de Ciència dels Materials i Enginyeria Metal·lúrgica, Universitat Politècnica de Catalunya-Barcelona Tech, C/ Colom 114, E-08222 Terrassa, Barcelona, Spain

*Corresponding author: jose.ignacio.velasco@upc.edu

Abstract

The present work deals with the preparation and characterization of improved fire-retardant ethylene-acrylate foams. A commercial formulation, usually employed in the cable industry sector, *Casico*, was modified using two different synergistic flame retardant (FR) systems: silica/zinc borate micro-sized particles (M) and montmorillonite/graphene nanoplatelets (N). The different composites were prepared by melt-blending and the foams by a compression-molding chemical foaming process (Casico-based foams). All Casico-based foams presented a mainly closed-cell structure. The presence of the nanoparticles system (N) promoted the formation of microcellular foams, with cell sizes lower than 100 μm, and narrow cell distributions. Nevertheless, when both flame retardant systems were added a higher cell collapse was noticed. Due to the foam's Casico-N structure and the presence of the stiff layered nanoparticles an increase of the temperature of β and α relaxations and specific loss modulus was registered for that foam respect to the Casico foam. In a general way, the Casico-based foams presented a thermal decomposition behavior similar to that of unfoamed Casico. Only a slight increase of the thermal stability of the step associated to the ionomer decomposition was observed respect to the Casico. Significant fire behavior improvements were observed for Casico-M-N foam. Specifically, this foam showed the lowest value of PHRR (peak of heat release rate), EHC (effective heat of combustion) and FIGRA (fire index growth rate), having therefore the lowest flammability, even lower than Casico unfoamed material.

Keywords: Flame retardancy, polymer foams, nanoparticles, DMTA, thermal stability, cone calorimeter.

1. Introduction

Traditionally, polymers containing halogen atoms such as polyvinyl chloride (PVC) have been widely used in applications that require good fire-resistance, such as in cable coating. Nevertheless, these materials produce corrosive and toxic gases as well as dense smoke during a fire, which raises concerns in terms of environmental and safety issues [1, 2]. Polyolefins, on the other hand, emit non-toxic and non-corrosive gases when burning and can be easily recycled. Furthermore, they display favourable characteristics for cable coating, such as excellent dielectric properties, a proper balance of physical and barrier performance, processability and low density. However, polyolefins are highly flammable and show significant dripping when burning [3].

Polymeric formulations based on ethylene acrylate copolymer-silicon-chalk have been developed in the last two decades as an alternative to the halogenated and high load magnesium hydroxide composites for cable insulation and jacket production [4-8]. The fire performance improvements attained with ethylene acrylate copolymer-silicon-calcium carbonate formulation have been assigned to an intumescent process [4] and the formation of a glassy layer in the surface due to migration of the silicon degradation products. The dispersion of both silicone elastomer and $CaCO_3$ in the polymer matrix seems to be decisive in the improvement of flame retardancy [7], together with the material's viscosity in the melt state. Particularly, viscosity of the material affects the transportation of volatile gases, eventual dripping, and the formation of the intumescent structure [9]. Huang et al [10], have show that the viscosity of this kind of flame retardant formulations changes not only with the temperature but also with the content of Ca-ionomers, that are formed during the thermal decomposition of the ethylene acrylate copolymer-silicon-chalk, and have studied the evolution of the Si/C ratio with temperature.

Karlsson et al [11], have studied the effect of nanofillers on the flame retardant properties of a polyethylene-calcium carbonate-silicone elastomer system. The authors found that the addition of an organically modified montmorillonite (MMT) to the mentioned system based on EBA and EMMA increased the flame retardant properties by reducing dripping and the heat release rate, which was related to an increase in melt viscosity. They concluded that, unlike the hydrated systems, the flame retardant properties of polyethylene-calcium carbonate-silicone elastomer formulations were dependent on the formation of a protective surface skin. The incorporation of a low content of nanoparticles as polymer flame retardants has also been studied in this kind

of polymer formulations [12-14]. The flame retardant effect of these nanoparticles has been attributed to char formation on top of the burning polymer, creating an efficient physical barrier that protects the substrate from heat and oxygen, slowing down the escape of flammable volatiles generated during polymer degradation [15]. It should also be mentioned that within the latest proposals for flame-retardant nanofillers, graphene nanoparticles have already proved to have the influence on polymer burning behavior [16, 17].

The interesting specific properties of polymer foams have caused a lot of interest in applications where solid materials can be replaced by lighter ones. However, the extensive uses of these materials in housing or transport applications have raised safety concerns. This is not surprising considering that these multiphase materials are composed of hydrocarbons and air, with a very low thermal inertia, making them prone to fast combustion [18]. Therefore, it is of great interest to study the flame retardancy of foamed materials, much less reported in literature than their unfoamed counterparts. Moreover, most of the work found in the literature related to the study of fire behavior of polymer foams is mainly focused on rigid and flexible polyurethane foams [19-23], only few dedicate their study on the fire behavior of polyolefin flame retardant foams [24-26].

With all these considerations in mind, this work intends to prepare, by using a chemical foaming process, foams of a modified commercial flame retardant polyethylene copolymer, and analyze the effects of such modifications on the cellular structure and final properties, particularly on the thermal-mechanical behavior, thermal stability and fire behavior, with the final goal of developing lightweight materials for structural applications where a good balance of specific mechanical properties and fire resistance is required.

2. Experimental

2.1. Materials

A polyolefin halogen-free flame retardant formulation, with the commercial name *Casico^{TM} FR4805*, manufactured by Borealis was used as base material. Casico is short for Calcium carbonate, Silicone elastomer and an acrylate containing (EBA) Copolymer. Casico formulations have approximately 30 wt.% of a $CaCO_3$, 5 wt.% of a polydimethylsiloxane (PDMS) and UV stabilization system [4]. This formulation has a density of 1.15 g/cm^3 and a melt flow index of 0.4 g/10 min.

Porofor® ADSC/M-C1 produced by Lanxess Energizing Chemistry, with an ADC content of 99.1%, a density of 1.65 g/cm^3 and a median particle size of 3.9 $\pm$ 0.6 μm was employed as chemical foaming agent. Different flame retardant fillers/additives were also incorporated into the Casico, namely: an amorphous precipitated silicon dioxide grade (S) of Rhodia-Solvay (commercial name: *Tixosil® 38*) with a median particle diameter of 15 μm, a typical surface area of 190 m^2/g and an apparent density of 2.2 g/cm^3; a zinc borate (ZB) of Borax (commercial name: *FirebrakeZB*) with a median particle size of 9 μm and a density of 2.8 g/cm^3; a montmorillonite (MMT) provided by Süd-Chemie (commercial name: *Nanofil SE3000*), organically-modified with dimetil-distearyl ammonium chloride, with a median particle size < 10 μm, a maximum surface area of 700 m^2/g and a density of 1.3 g/cm^3. Among the several carbon substrates available as potential FR additives [17, 27], a commercial grade of graphene nanoplatelets (GnP) was used. It was supplied by XG Sciences, Inc. (commercial name: *xGnP-M-15*), with an average diameter of 15 mm and a thickness of 6-8 nm, with a typical surface area of 120-150 m^2/g and a density of 2.2 g/cm^3.

2.2. Samples preparation

2.2.1. Compounding and molding

The several Casico based composites were prepared by melt-compounding the different components using *a Brabender Plasti-Corder* static mixer, at a temperature and screw speed of 165 ºC and 30-60 rpm respectively, with a mixing time of 5 min. Table 1 presents the composition of the several composites. All Casico formulations contain 3.5 parts per hundred of polymer of the chemical blowing agent (ADC).

In order to prepare the foaming precursors, the compounded composites were quickly placed, after removing from the Brabender mixer, into circular molds with a diameter of 74 mm and thickness of 3.5, and compression-molded by heating at 160 ºC applying a pressure of 40 bar using a hot-plate press *IQAP-LAP PL-15*.

Circular-shaped Casico discs without ADC of 74 mm diameter with 3.5 and 6 mm thickness were also prepared.

2.2.2. Foaming

The compression-molded foaming precursors were allowed to freely foam by the thermal decomposition of the blowing agent at a typical temperature of 200 ºC during a

minimum of 10 to a maximum of 25 min by placing the samples inside a closed chamber between the hot plates of the press. The produced foamed composites showed a final expansion ratio (ER), defined as the ratio between the density of the solid base composite and the density of the foam, between 2.1 and 2.5. Specimens were directly cut from the foamed materials and the solid skins generated during foaming removed prior to their characterization.

2.3. Characterization

2.3.1. Cellular structure

The density of both unfoamed and foamed composites was measured according to ISO 845. Relative density (ρ_r) was determined by dividing the density of the foamed sample by the value of the unfoamed one. The cellular structure of the foams was analyzed by means of scanning electron microscopy (SEM) using a *JEOL JSM-5610* microscope. Samples were prepared by cryogenically fracturing using liquid nitrogen and sputter depositing at their surfaces a thin layer of gold. The average cell size (ϕ) and cell density (N_f) were determined using the intercept counting method [28]. Two cell sizes were determined according to the direction of foam growth: ϕ_{VD}, where VD is the vertical foam growth direction and ϕ_{WD} (WD: width direction). The cell aspect ratio (AR) was determined as the ratio between both cell sizes, i.e., $AR = \phi_{VD}/\phi_{WD}$.

2.3.2. Dynamic mechanical thermal analysis

Dynamic mechanical thermal analysis (DMTA) was used to observe differences in the tanδ and storage modulus of foams and unfoamed Casico. A *DMA Q800* from *TA Instruments* was used and calibrated in a single cantilever configuration. The experiments were performed from -20 to 150 ºC, under a liquid nitrogen atmosphere, at a heating rate of 2ºC/min and frequency of 1 Hz, applying a dynamic strain of 0.02%. Test specimens were prepared in a rectangular shape with a typical length of 35.5 ± 1.0 mm, width of 12.5 ± 1.0 mm and thickness of 3.5 ± 0.5 mm.

2.3.3. Thermal stability

The thermal stability of the composites was characterized by means of thermogravimetric analysis (TGA) using a *TGA/DSC1 Mettler Toledo Star System* analyzer by placing unfoamed and foamed samples with an average weight of 10 and 7

mg respectively, applying a constant heating rate of 10 ºC/min from 30 to 1000 ºC under a constant flow of 30 ml/min of nitrogen.

2.3.4. Fire behavior

The heat release rate (HRR) during combustion was determined using a cone calorimeter (*INELTEC*, Spain) according to ISO 5660 standard procedure. Unfoamed and foamed circular-shaped specimens with a diameter and thickness of 73 $\pm$ 2 mm and 6 $\pm$ 0.5 mm respectively, were irradiated with a constant heat flux of 50 kW/m^2. Fire behavior parameters such as time to ignition (TTI), peak of the heat release rate (PHRR), total heat emitted (THE), effective heat of combustion (EHC), determined by dividing the THE by the sample mass loss, and fire growth rate (FIGRA), determined by dividing the PHRR by the time to the PHRR, were measured.

3. Results and discussion

3.1. Cellular structure

Figure 1 shows characteristic SEM micrographs of the different Casico-based foams. Firstly, SEM micrographs show, qualitatively, that all foams presented a mainly closed-cell structure. Nevertheless, when both flame retardant systems were present, a higher cell collapse was noticed. Secondly, it can be concluded that the average cell size decreased with the presence of MMT and GnP nanoparticles.

With the aim of quantifying the qualitative results previously mentioned, several characteristics of the cellular structure were measured (see values presented in Table 2). Furthermore, in order to analyze the homogeneity of the cellular structure, the cell size distribution of all foams was evaluated. Figure 2 shows the corresponding histograms.

In general, like it was previously mentioned, foams presented an expansion ratio (ER=1/ρ_r, where ρ_r is the relative density (ρ_{foam}/ρ_{solid})) between 2.1 and 2.5, being the Casico-M the formulation with lower relative density or higher expansion ratio.

Comparatively, the addition of small concentrations of nanofillers (1 wt% of MMT and 1 wt% of GnP) into the Casico formulation led to microcellular foams with cell sizes (ϕ) lower than 100 μm with a cell reduction of approximately 260 % (see Table 2) and a cell density (N_f) 30 times higher respect to the Casico foam. This cell size reduction and the narrow cell distributions (see Figure 2) were attributed to the well-known effective heterogeneous cell nucleation effect promoted by the layered nanoparticles [29-32].

On the other hand, an opposite effect was observed in the presence of more traditional microsized particles (silica and zinc borate), i.e., the Casico-M flame retardant system presented a cell size increase respect with the Casico foam and the lowest cell density. Furthermore, a preferred orientation of the cell structure in the vertical direction and a wider cell size distribution was observed for Casico-M foam (see Figure 2).

Finally, the combination of both flame retardant systems (Casico-M-N), although apparently helped to reduce the cell size of foams, promoted the formation of a more collapsed cell structure with much lower aspect ratios ($\phi_{VD} << \phi_{WD}$, thus AR<1). The collapse of cells during cell growth could indicate a different viscoelastic behavior due to the higher content of fillers and different interaction between fillers, gas and polymer matrix [25]. The results are an indication of the difficult task of foaming a material with high amount of fillers of different nature ($CaCO_3$, ZB, S, MMT and GnP).

3.2. Dynamic mechanical thermal analysis (DMTA)

The DMTA scans from -20 to 140 ºC of unfoamed Casico and foamed formulations are presented in Figure 3. It should be mentioned that PDMS thermomechanical transition, normally registered close to -120ºC [33] and the γ relaxation (glass temperature), of the polyethylene based material, usually observed between -90 and -130 ºC [34], were not analyzed in the present study.

All DMTA runs showed three thermomechanical transitions. The temperature, at which tan δ displays a maximum, corresponds to a transition or a relaxation of the polyethylene based material. For the unfoamed Casico the maximum values observed at 7 ºC and 56.3 ºC were related with two typical relaxations of ethylene based polymers, i.e., β relaxation associated with the amorphous phase and α relaxation related to the crystalline one [34]. The third maximum registered at 120 ºC was attributed to the melting of the crystalline phase of the EBA copolymer.

The Casico-based foams presented the same average behavior of unfoamed Casico (see Figure 3). Notwithstanding, β relaxation was found to slights decrease in all Casico-based foams and that seems to be due to the foaming process itself and related to the cellular structure of the samples. Particularly, in the foam sample with presence of MMT and GnP nanoparticles (Casico-N) the β relaxation appeared at the highest temperature (3.6 ºC). Furthermore, the α relaxation of this foam was also registered at

higher temperature, even more than the Casico unfoamed sample. This fact could be due to the presence of the layered nanoparticles, which hindered the rotation of the EBA molecules [35]. Additionally, the intensity of thermal transitions when the nanoparticles (Casico-N) are present is lower, as can be seen in Figure 3, which confirms the lower ability to dissipate energy through molecular motion of this foam.

As was expected the storage modulus (E') of foams decreased considerably when compared to the unfoamed Casico base material. However, if we compare the specific values the differences are lower (see Table 3).

Casico foam presented the lowest values of E', which could be due to a combined effect of the lower density and the absence of the flame retardant fillers, stiffer than the polymer matrix. On the other hand, Casico-N foam presented the higher specific storage modulus, respect to the remaining foams. This fact could be attributed the higher foam density, high cell density and the presence of stiffer nanoparticles. Comparatively, Casico-M foam presented a higher specific storage modulus than Casico-M-N foam; this fact was related to the collapsed cellular structure of this foam (see Figure 1d).

3.3. Thermal stability

Figure 4 illustrates the evolution of the weight loss with temperature and respective derivative curves (dTG curves) of unfoamed Casico, Casico foam and Casico-based flame retardant foams. The data, including the temperature corresponding to the 5%, 25% and 50% of weight loss and to the maximum decomposition of each step and respective weight loss, are collected in Table 4.

As is possible to see in Figure 4, the thermal degradation of unfoamed Casico occurred in two main weight loss stages, while Casico-based foams decomposed in three main stages. This difference is attributed to the presence of the foaming agent in the Casico-based foams. ADC (foaming agent) decomposes around 200-220 ºC, generating a gas mixture of N_2, CO and CO_2, as well as solid residues [36].

The following two weight loss stages (step 2 and step 3, see Table 4) occurred in all formulations and are typical of unfoamed Casico [4, 5]: between 300 and 500 ºC, the higher weight loss stage (step 2) was registered and related to ethylene copolymer pyrolysis with the formation of butene and carboxylic acid groups:

$$\text{Polymer} - COOC_4H_9 \rightarrow \text{Polymer} - COOH + CH_2 = CH - CH_2 - CH_3 \uparrow \quad (1)$$

These acid groups with the presence of calcium carbonate are instead converted to carboxylate. Ionomers are then formed between the carboxylates originating from the acidic groups and calcium ions originating from $CaCO_3$:

$$2Polymer - COOH + CaCO_3 \rightarrow (Polymer - COO)_2Ca^{2+} + CO \uparrow + H_2O \uparrow \quad (2)$$

This reaction contributes to the flame retardant mechanism in two ways. First, it leads to the formation of foaming gases at a lower temperature than the normal degradation of the polymer backbone. This means that a heat-insulating layer is formed at an earlier stage. In addition, the gases formed are inert and may have a suffocating effect. The formation of ionomers between carboxylate groups and calcium ions is a second important contribution. This introduces crosslinks in the melt increasing its viscosity thus stabilizing the initially formed intumescent structure [4].

The last stage (step 3) was mainly related with the thermal decomposition of the silicone and calcium carbonate that produces a calcium silicate (Ca_2SiO_4) and a calcium oxide (CaO). The calcium silicate could be formed according to the reaction sequence equations (3) to (5) presented below:

$$PDMS \rightarrow SiO_x + (VOC \uparrow) \ (> 500ºC) \quad (3)$$

$$CaCO_3 \rightarrow CaO + CO_2 \uparrow \ (>600ºC) \quad (4)$$

$$CaO + SiO_x \rightarrow Ca_2SiO_4 \ (> 600 \ ºC) \quad (5)$$

As was previously reported [4, 5], calcium silicate is formed through a sintering reaction between CaO and SiO_2. Since the amount of CaO is higher than SiO_2, CaO is also present in the final residue.

In general, the incorporation of the mentioned flame retardant systems (M and N) into the Casico-based foams did not show significant changes in terms of Casico thermal stability, except in the third and last decomposition step, related with the silicone and $CaCO_3$ thermal decomposition. All Casico-based foams presented a higher value of the temperature associated to the maximum rate of decomposition (T_{max}, step 3) respect to the unfoamed Casico formulation. This slight increase could be related with the more insulating residue cellular structure involved in this foam thermal decomposition stage.

It must be said that Casico-M-N foam showed the higher inorganic residue content followed by the Casico-M foam, which is not surprising, due to the higher inorganic content of these formulations.

3.4. Fire behavior

By reducing Casico density to less than half (ER=2.4), using a chemical foaming process it was possible to observe that Casico foam showed a decrease of the total heat emitted (THE) and of the ignition (TTI) and combustion (t_c) times respect to the unfoamed Casico. This fact is related to the lower volume fraction of polymer and porous cellular structure in Casico under the high radiant heat flux (50 kW/m^2) employed during the cone calorimeter tests. It is well known that these parameters, among others, depend on sample's dimension, density and geometry, as well as, of the employed radiant heat flux and material's thermal properties during combustion, i.e., thermal conductivity and heat capacity [37]. Particularly, the pronounced decreased of the TTI of foams could be related to their higher specific area, which leads to a higher oxygen access during the ignition stage.

Unfoamed Casico, Casico and Casico-M foams showed a similar burning behavior. As can be seen in Figure 5, all these samples showed a typical steady state burning marked by a shoulder followed by an increase of HRR until reaching a maximum (PHRR), typical of intermediate thick samples without efficient char layer formation [38]. It must be said that, although these samples presented similar burning behaviors, the Casico-M foam showed a more cohesive layer, lower values of PHRR and effective heat of combustion (EHC) and a higher value of TTI. Nevertheless, no characteristic residue-formation was observed. This fact, could be related mainly with the mode of action of the zinc borate flame retardant additive, which dehydrates endothermically, absorbing heat from the flame and diluting the oxygen and the combustible gases and promotes also the formation of a glassy char that protects the polymer from the combustion zone [39, 40].

A different burning behavior was observed for Casico-N and Casico-M-N foams. After ignition, these foams presented a small peak or a quasi-static HRR followed by a maximum (PHRR), which is indicative of an improved barrier efficiency. This fact could be related with the presence of a small amount of nanoparticles, since during combustion these nanofillers tend to migrate to the material's surface, improving the fire resistance by generating a more protective layer [41]. A higher flame resistant enhancement was produced by the combination of the two FR systems (M and N), since the observed quasi-static HRR behavior was prolonged respect to Casico-N foam. Unfortunatly, the physical barrier was not completly effective because the HRR curves

of both foams showed, as previously mentioned, a PHRR after the quasi-static HRR, indicating a further decomposition of the material.

The analysis of the HRR curves of Casico-N and Casico-M-N foams are sustained by the photos made during and after the CC tests (see Figure 6). Althought gas could escape from the lateral of the samples (related with the PHRR), a more cohesive layer could still be observed in those samples.

It should be noted that all tested foams did not suffer a significant structure collapse before and after ignition due to the higher content of inorganic fillers and the high melt strength of Casico formulation. The formation of ionomers during combustion between carboxylate groups and calcium ions of the Casico formulation introduces crosslinks in the melt increasing its viscosity [4].

All Casico foams presented approximately 33% of weight residue (similar to unfoamed Casico), except Casico-N-M foam that showed an increase of 3%. This fact, could indicate that, except for Casico-M-M foam, no significant improvements in the condensed-phase mecanisms occured during the combustion of the Casico FRs foams respect with the Casico foam. However, this slight increment could also be due to slight differences in composition.

In order to be abble to compare the values of THR of Casico-based foams with the unfoamed Casico, without the effect of the mass sample, normalized THR values (THR_{norm}) were determined used the followed equation:

$$THR_{norm} = THR_{sample} \cdot mass_{Casico,\ unfoamed} / mass_{sample} \quad (6)$$

It should be mentioned that this normalized parameter should not be considered a characteristic parameter of the material, but it have to be used to analyze possible variations of THR foam curves regarding to the unfoamed Casico one.

Casico-M-N values of THR_{norm} (Figure 7) and EHC were lower than those determined for the remaining samples, probably due to the combined mechanisms of action of both flame retardant systems. Furthermore, Casico-M-N showed the lowest value of FIGRA, having therefore the lowest flammability, even lower than Casico unfoamed material.

Conclusions

The incorporation of MMT and GnP into the Casico base formulation promoted the formation of foams with finer and homogeneous cellular structures with micrometric

cell sizes. Nevertheless, a more collapsed cellular structure was observed in the Casico foamed formulation when both flame retardant systems (Casico-M-N) were added.

The foaming process seemed to be the cause of EBA's β relaxation transition reduction observed in all Casico-based foams respect to the unfoamed Casico. Nonetheless, due to the layered nanoparticles presence and the thinner and more homogeneous cellular structure of Casico-N an increase of the α and β relaxation transitions and specific loss modulus was registered for that foam respect to the Casico foam.

In general, no significant improvement in terms of Casico foam's thermal stability was observed with the incorporation of the flame retardant system (M and N). However, an increase of the maximum rate of decomposition associated to the ionomer decomposition was observed for all foams respect to the unfoamed Casico.

Enhanced flame retardancy with a significant reduction in PHRR was observed when nanoparticles were incorporated into the Casico foamed formulation. A more cohesive protective layer was formed during the cone calorimeter test of Casico-N and Casico-M-N foams. This fact was related to the well-known migration of these particles to the material's surface during combustion. The fire behavior improvement was even more significant when both flame retardant systems (M and N) were present, due to the combined mechanisms of action of both flame retardant systems. Casico-M-N showed the lowest value of PHRR, EHC and FIGRA, having therefore the lowest flammability, even lower than Casico unfoamed material.

Acknowledgements

The authors would like to acknowledge the Spanish Ministry of Economy and Competitiveness for the financial support of project MAT2014-5613.

References

1. P. Carty, S. White, Polym. Polym. Compos. 6 (1998) 33-38.

2. A.A. Stec, T.R. Hull, in: C.A. Wilkie, A.B. Morgan (Eds), Fire retardancy of polymeric materials, 2nd ed., CRC Press, New York, 2010, p. 456.

3. R.J. Schwarz, in: W.C. Kuryla, A.J. Papa (Eds), Flame Retardancy of Polymeric Materials, Marcel Dekker, New York, 1973, p. 83.

4. A. Hermansson, T. Hjertberg, B.A. Sultan, Fire Mater. 27, (2003) 51-70.

5. A. Hermansson, T. Hjertberg, B.A. Sultan, Fire Mater. 29 (2005) 407-426.

6. J. Yang, S. Zhou, B. You, L. Wu, High Perform. Polym. 17 (2005) 85-102.

7. A. Hermansson, T. Hjertberg, S.A. Sultan, J. Appl. Polym. Sci. 100 (2006) 2085-2095.

8. R.H. Krämer, P. Blomqvist, P.V. Hees, U.W. Gedde, Polym. Degrad. Stab. 92 (2007) 1899-1910.

9. A. Lundgren, T. Hjertberg, B.A. Sultan, J. Fire Sci. 25 (2007) 287-319.

10. N. Huang, Y. Wang, J. Fire Sci. 27 (2009) 235-264.

11. L. Karlsson, A. Lundgren, J. Jungqvist, T. Hjertberg, Fire Mater. 35 (2011) 443-452.

12. J. W. Gilman, Appl. Clay Sci. 15 (1999) 31-49.

13. D. Wang, K. Echols, C.A. Wilkie, Fire Mater. 29, (2005) 283-294.

14. P. Kiliaris, C.D. Papaspyrides, R. Pfaendner, Macrom. Mater. Eng. 296 (2011) 617-629.

15. P. Kiliaris, C.D. Papaspyrides, Prog. Polym. Sci. 35 (2010) 902-958.

16. B. Dittrich, K.-A. Wartig, R. Mülhaupt, B. Schartel, Polymers 6 (2014) 2875-2895.

17. B. Dittrich, K.-A. Wartig, D. Hofmann, R. Mülhaupt, B. Schartel, Polym. Degrad. Stabil. 98 (2013) 1495-1505.

18. M. Modesti, A. Lorenzetti, in: C.A. Wilkie, A.B. Morgan (Eds), Fire retardancy of polymeric materials, 2nd ed., CRC Press, New York, 2010, p. 763.

19. M. Zhang, J. Zhang, S. Chen, Y. Zhou, Polym. Degrad. Stabil. 110 (2014) 27-34.

20. L. Gao, G. Zheng, Y. Zhou, L. Hu, G. Feng, M. Zhang, Polym. Degrad. Stabil. 101 (2014) 92-101.

21. A. Lorenzetti, S. Besco, D. Hrelja, M. Roso, E. Gallo, B. Schartel, M. Modesti, Polym. Degrad. Stabil. 98 (2013) 2366-2374.

22. M. Thirumal, N. K. Singha, D. Khastgir, B.S. Manjunath, Y.P. Naik, J. Appl. Polym. Sci. 116 (2010) 2260-2268.

23. L. Ye, X. Y. Meng, X. Ji, Z. M. Li, J. H. Tang, Polym. Degrad. Stabil. 94 (2009) 971-979.

24. V. Realinho, L. Haurie, M. Antunes, J. I. Velasco, Comp. B – Eng. 58 (2015) 553-558.

25. S. Román-Lorza, M.A. Rodríguez-Pérez, J.A De Saja, J. Zurro, J. Cell. Plast. 46 (2010) 259-279.

26. S. Roma-Lorza, M.A. Rodriguez Perez, J.A.D Saez, Cell. Polym. 28 (2009) 249-558.

27. Dittrich, K.-A. Wartig, D. Hofmann, R. Mülhaupt, B. Schartel, Polym. Adv. Technol. 24 (2013) 916-926.
28. G. Sims, C. Khunniteekool, Cell. Polym., 13 (1994)137-146.
29. M. Antunes, J. I. Velasco, V. Realinho, J. Nanomater. (2010), Article ID 306384.
30. W. Zhai, J. yu, L. Wu, W. Ma, J. He, Polymer 47 (2006) 7580-7589.
31. R.B. McClurg, Chem. Eng. Sci. 59 (2004) 5779-5786.
32. J.J. Feng, C.A. Bertelo, J. Rheol. 48 (2004) 439-462.
33. M.V. Pergal, J.V. Dzunuzdvic, R. Poreba, D. Micic, P. Stefanov, L. Pezo, M. Spirkova, Express Polym. Lett. 7 (2013) 806-820.
34. E. Passaglia, S. Coiai, G. Taburoni, L. Fambri, V. Pagani, M. Penco, Macromol. Mater: Eng. 289 (2004) 809-817.
35. K.S. Kumar, C.P. Nair, K.N. Ninan, J. Appl. Polym. Sci. 107 (2008) 1091-1099.
36. H. Hurnik, in: H. Zweifel, R. Maier, M. Schiller (Eds.) Chemical Blowing Agents. Plastics Additives Handbook, 6th ed., Hanser, Munich, 2009.
37. P. Patel, T.R. Hull, A.A. Stec, R.E. Lyon, Polym. Adv. Technol. 22 (2011) 1100-1107.
38. B. Schartel, in: C.A. Wilkie, A.B. Morgan (Eds), Fire retardancy of polymeric materials, 2nd ed., CRC Press, New York, 2010, p. 398.
39. Y. Yang, X. Shi, R. Zhao, J. Fire Sci. 17 (1999) 355-361.
40. A. Genovese, R.A. Sanks, Polym Deg. Stabil. (2007) 2-13.
41. M. Modesti, A. Loerenzetti, S. Besco, D. Hrelja, S. Semenzato, R. Bertani, R.A. Michelin, Polym. Deg. Stabil. 93 (2008) 2166-2171.

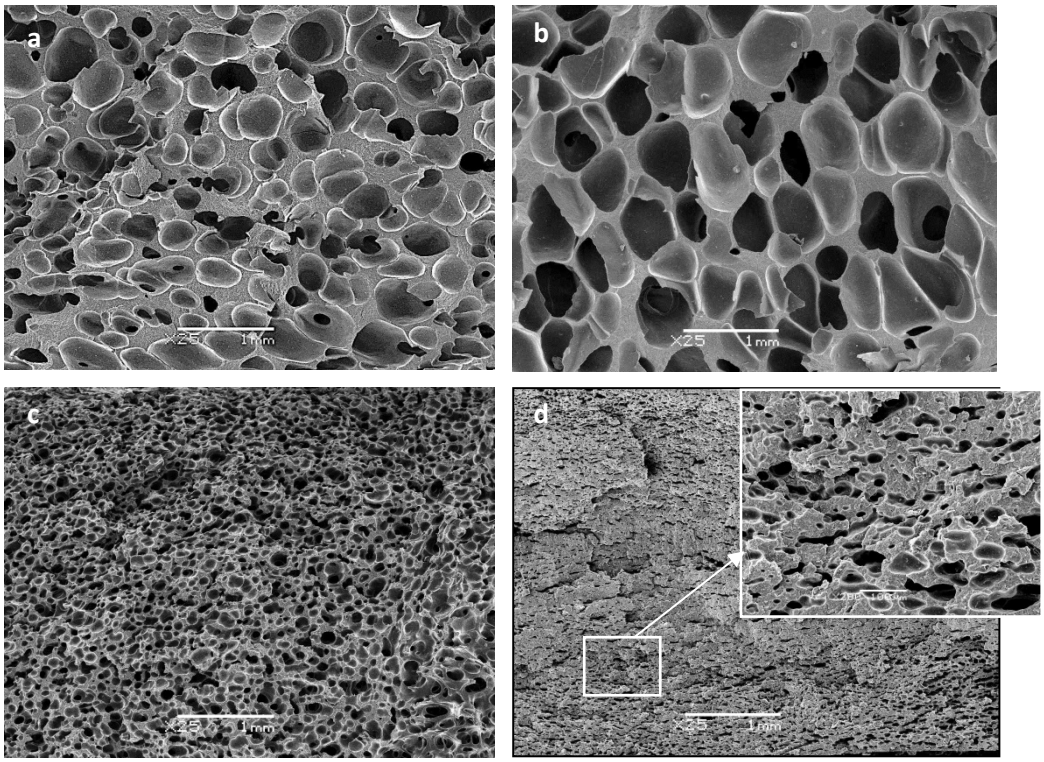

Figure 1. Characteristic SEM micrographs of foamed formulations. a) Casico, b) Casico-M, c) Casico-N and d) Casico-M-N.

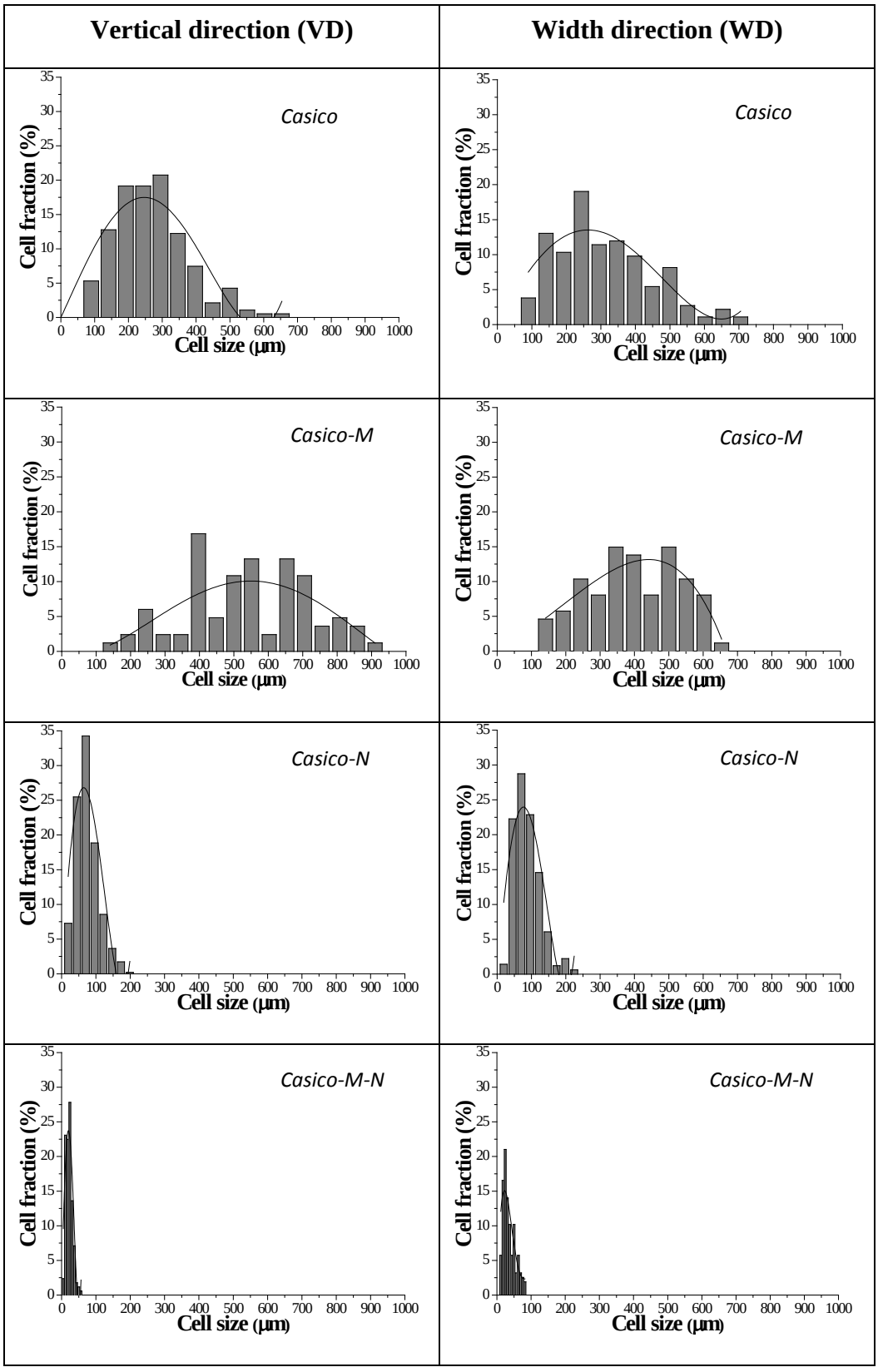

Figure 2. Cell size distributions in vertical and width direction of Casico-based foams.

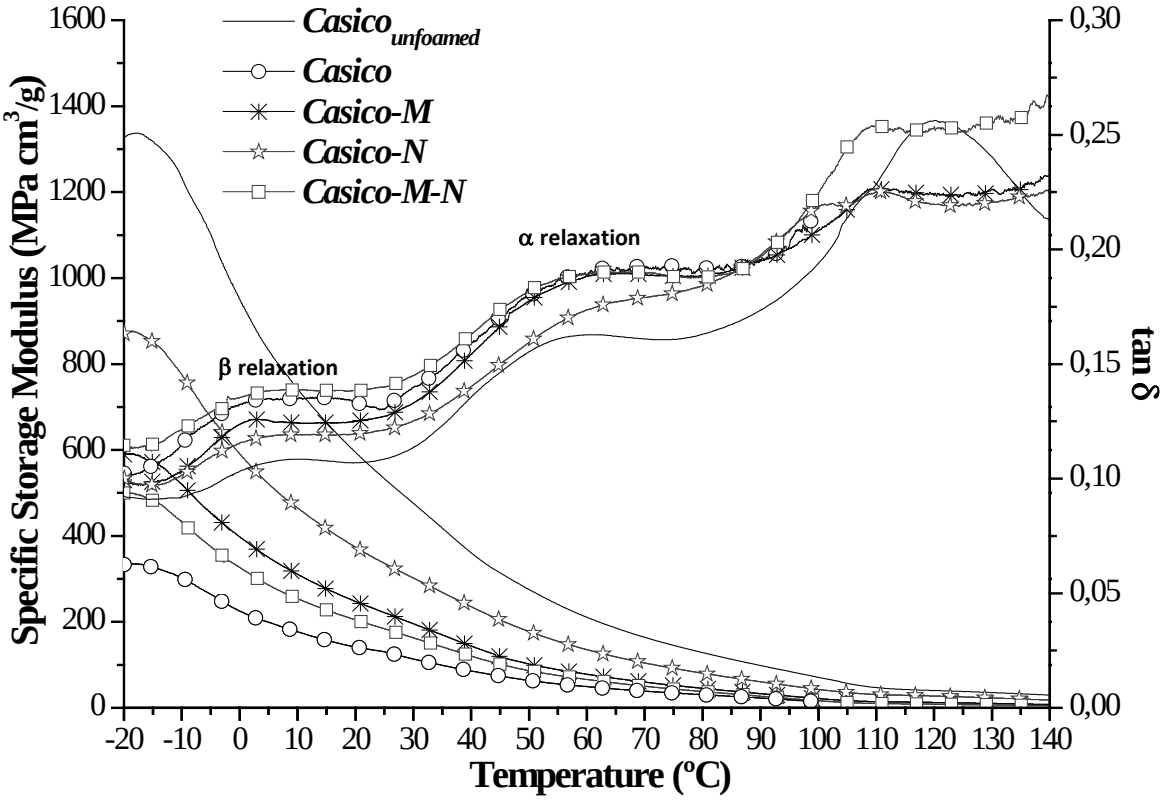

Figure 3. Specific storage modulus (E') and tan δ of unfoamed Casico and Casico-based foams.

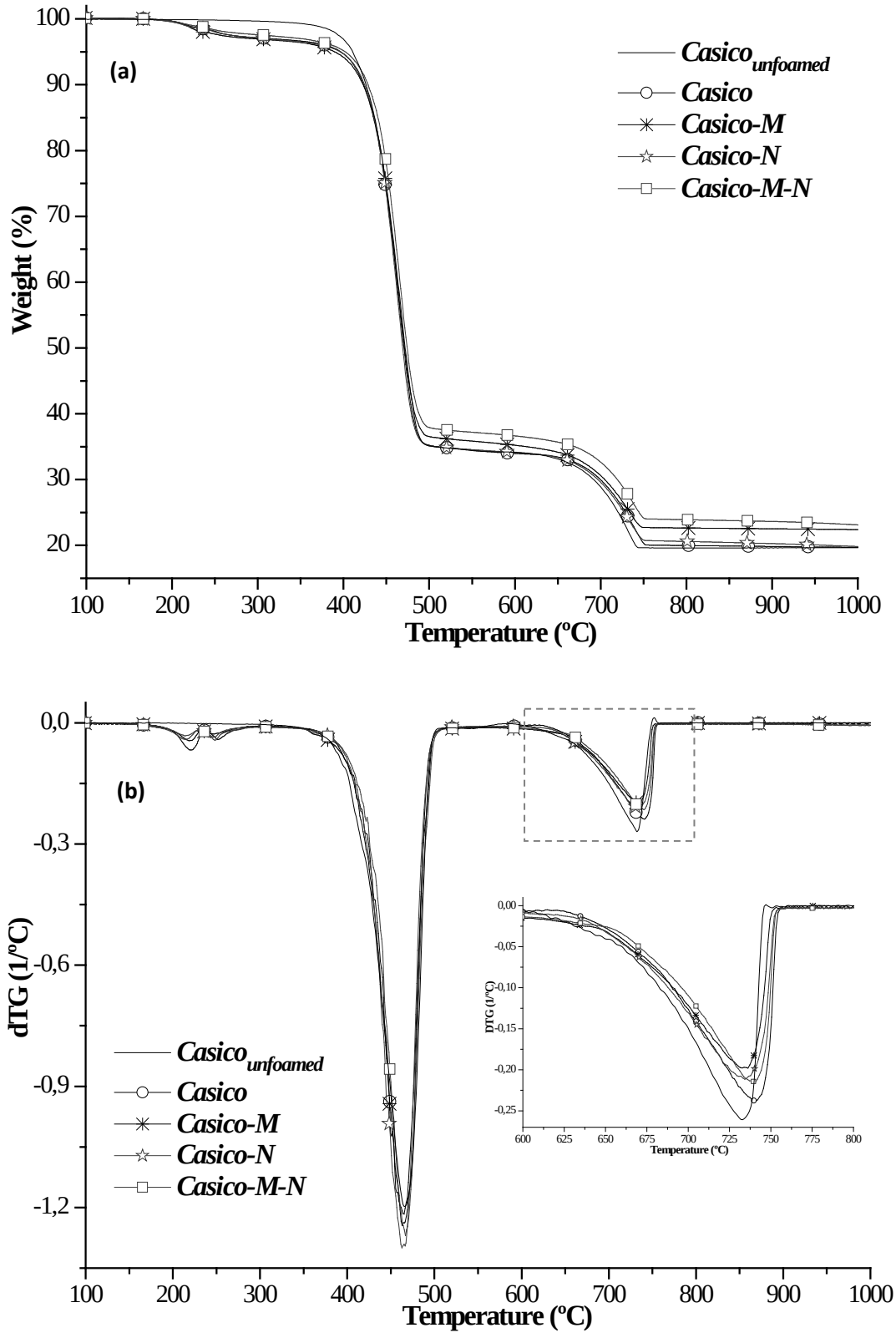

Figure 4. a) Thermogravimetric weight loss and (b) first derivative (dTG) curves for Casico, and Casico foams obtained at 10ºC/min under nitrogen atmosphere.

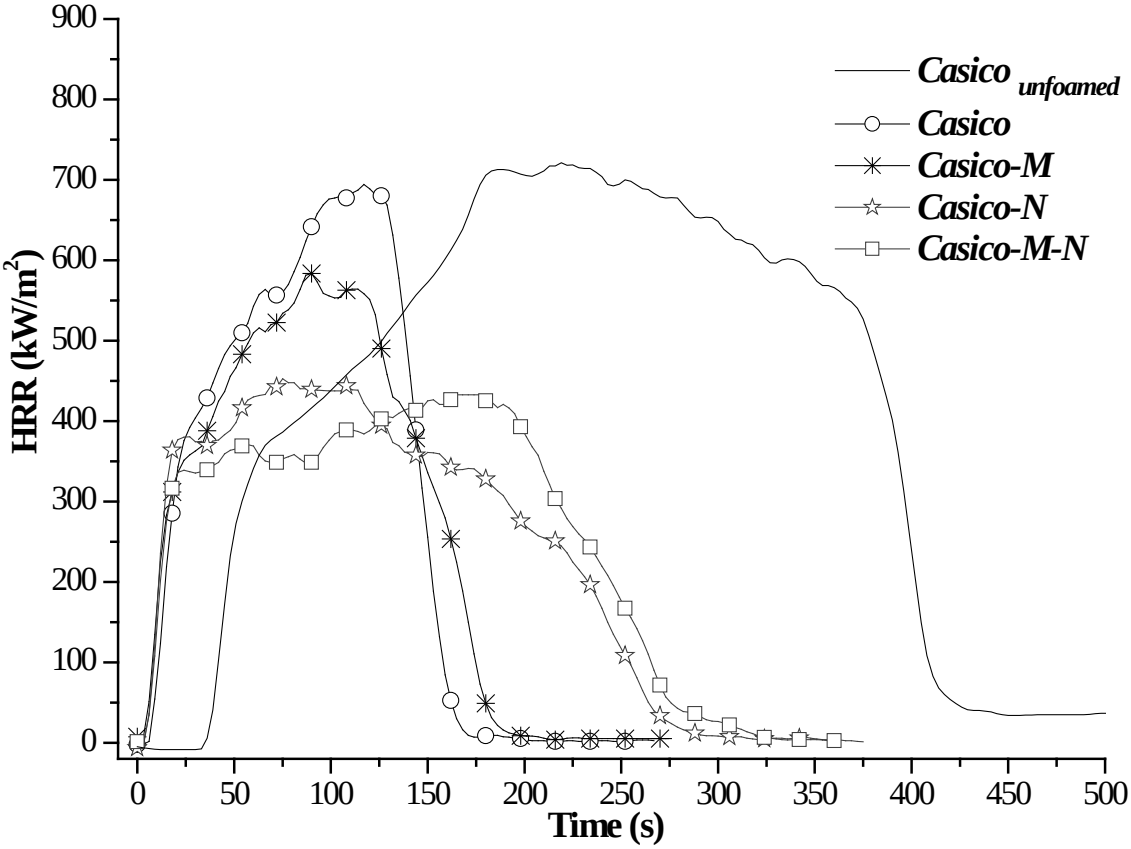

Figure 5. Typical cone calorimeter curves of both unfoamed Casico and Casico-based foams.

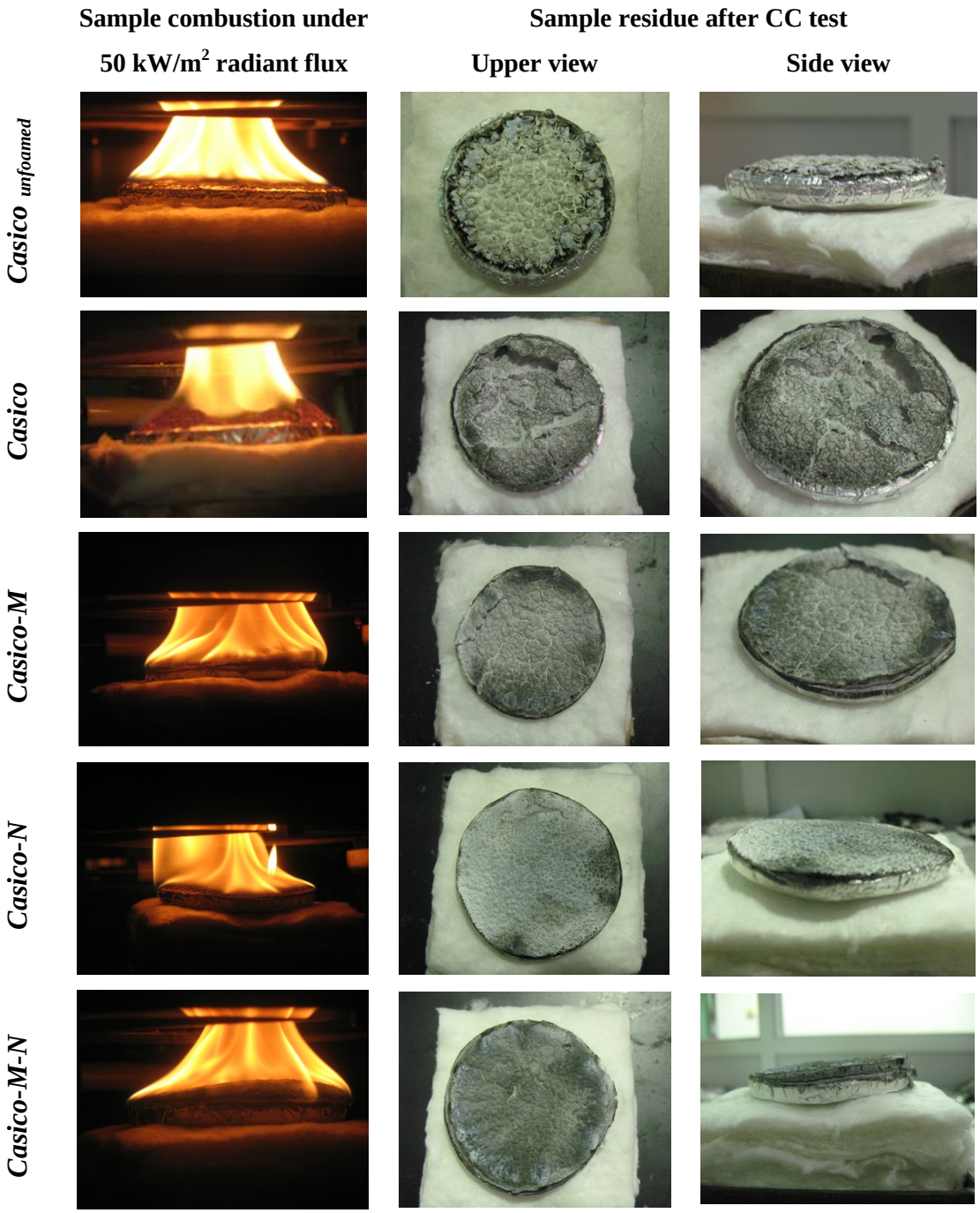

Figure 6. Unfoamed Casico and Casico-based foams during and after cone calorimeter (CC) test.

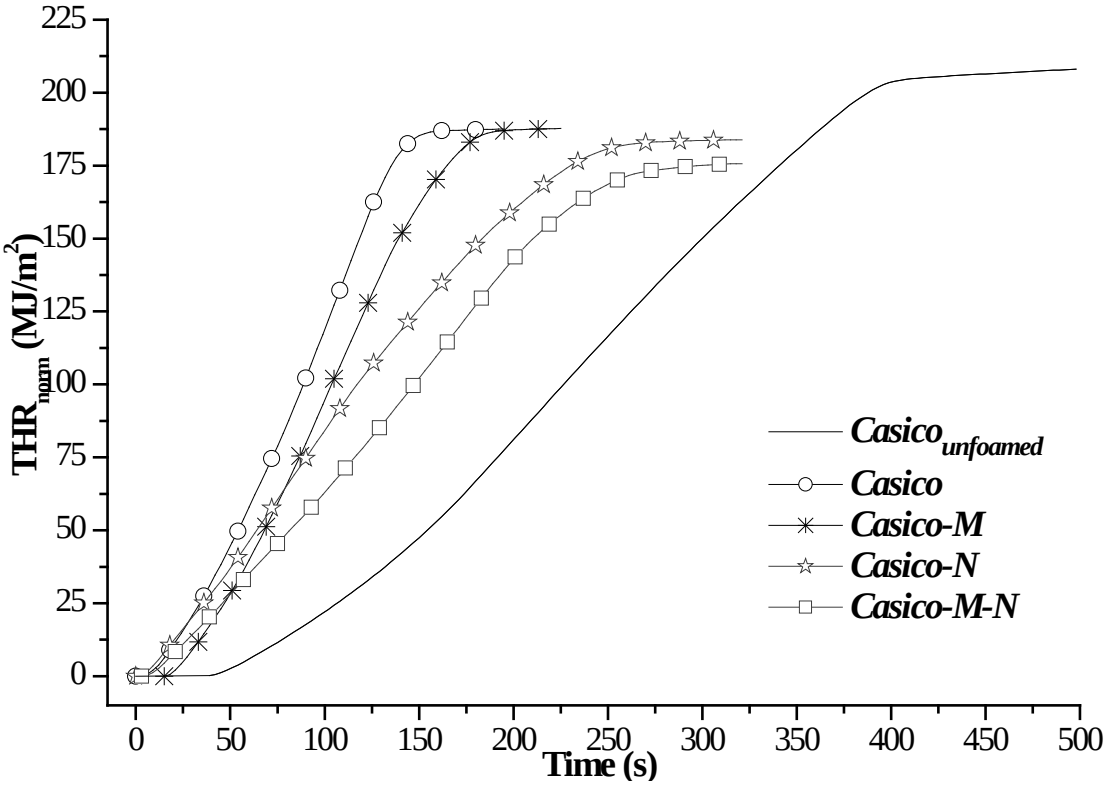

Figure 7. THR_{norm} curves (normalized THR curves) as a function of time of unfoamed Casico and Casico-based foams.

Table 1. Composition of the several composites.

Material code	**M (wt.%)**		**N (wt.%)**	
	S	**ZB**	**MMT**	**GnP**
Casico	-	-	-	-
Casico-M	2	2	-	-
Casico-N	-	-	1	1
Casico-M-N	2	2	1	1

Table 2. Relative density and cellular structure characterization results of Casico-based foams.

Foam code	ρ_r	**ER**	ϕ_{VD} **(μm)**	ϕ_{WD} **(μm)**	**AR**	N_f **(cells/cm^3)**
Casico	0.42	2.4	268 ± 19	310 ± 15	0.86	9.06×10^4
Casico-M	0.40	2.5	538 ± 29	397 ± 23	1.36	3.18×10^4
Casico-N	0.48	2.1	73 ± 9	87 ± 9	0.84	1.19×10^6
Casico-M-N	0.42	2.4	22 ± 2	36 ± 1	0.62	9.06×10^7

Table 3. Thermomechanical transitions, storage modulus and specific storage modulus of unfoamed Casico and Casico-based foams.

Material code	**β relaxation (ºC)**	**α relaxation (ºC)**	**E' (MPa) at 20ºC**	**Specific E' (MPa.cm^3/g) at 20ºC**
Casico $_{unfoamed}$	7.0	56.3	669	594
Casico	1.7	55.0	68	142
Casico-M	1.9	56.2	114	247
Casico-N	3.6	58.2	218	374
Casico-M-N	2.0	55.4	94	205

Table 4. Characteristic temperature and weight loss of unfoamed Casico and Casico-based foams obtained from thermogravimetric analysis.

Material code	**$T_{5\%}$ (ºC)**	**$T_{25\%}$ (ºC)**	**$T_{50\%}$ (ºC)**	**T_{max} (ºC)**			**Weight loss (%)**		
				Step 1	**Step 2**	**Step 3**	**Step 1**	**Step 2**	**Step 3**
Casico $_{unfoamed}$	410	450	472	-	466	730	-	65.7	14.6
Casico	397	449	471	218	463	742	3.2	63.1	14.1
Casico-M	391	450	471	221	465	732	3.2	61.5	13.0
Casico-N	396	448	469	215	463	735	3.0	63.1	14.2
Casico-M-N	403	453	475	214	468	741	3.0	60.6	13.7

Table 5. Sample caracteristics and cone calorimeter results of unfoamed Casico and Casico-based foamed materials.

Material code	**TTI (s)**	**t_{PHRR} (s)**	**PHRR (kW/m^2)**	**Residue (%)**	**THE_{norm} (MJ/m^2)**	**EHC (MJ/kg)**	**FIGRA ($kW.m^{-2}.s^{-1}$)**
Casico $_{unfoamed}$	33	213	736	33.7	208.0	42.9	3.5
Casico	1	114	695	33.0	187.5	40.2	6.9
Casico-M	9	99	595	33.4	187.7	36.1	6.0
Casico-N	1	72	461	33.8	184.3	37.1	6.5
Casico-M-N	1	147	433	36.1	175.9	34.2	3.0